MIT Open Access Articles

Designing microbial consortia with defined social interactions

The MIT Faculty has made this article openly available. ***Please share*** how this access benefits you. Your story matters.

Citation	Kong, Wentao et al. "Designing Microbial Consortia with Defined Social Interactions." Nature Chemical Biology 14, 8 (June 2018): 821–829
As Published	https://doi.org/10.1038/s41589-018-0091-7
Publisher	Nature Publishing Group
Version	Author's final manuscript
Citable link	http://hdl.handle.net/1721.1/119451
Terms of Use	Creative Commons Attribution-Noncommercial-Share Alike
Detailed Terms	http://creativecommons.org/licenses/by-nc-sa/4.0/

Massachusetts Institute of Technology

DSpace@MIT

Designing Microbial Consortia with Defined Social Interactions

Wentao Kong[1,2], David R. Meldgin[2,3], James J. Collins[5,6,7,*], and Ting Lu[1,2,3,4,*]

Department of Bioengineering[1], Carl R. Woese Institute for Genomic Biology[2], Department of Physics[3], Center for Biophysics and Quantitative Biology[4], University of Illinois at Urbana-Champaign, Urbana, IL 61801, USA. Institute for Medical Engineering and Science, Department of Biological Engineering, and Synthetic Biology Center[5], Massachusetts Institute of Technology; Broad Institute of MIT and Harvard[6], Cambridge, MA 02142, USA; Wyss Institute for Biologically Inspired Engineering[7], Harvard University, Boston, MA 02115, USA

Correspondence and requests for materials should be addressed to T.L. (luting@illinois.edu) J.J.C. (jimjc@mit.edu).

Abstract

Designer microbial consortia are an emerging frontier in synthetic biology that enables versatile microbiome engineering. However, the utilization of such consortia is hindered by our limited capacity in rapidly creating ecosystems with desired dynamics. Here we present the development of synthetic communities through social interaction engineering that combines modular pathway reconfiguration with model creation. Specifically, we created six two-strain consortia with each possessing a unique mode of interaction, including commensalism, amensalism, neutralism, cooperation, competition and predation. These consortia follow distinct population dynamics with characteristics determined by the underlying interaction modes. We showed that models derived from two-strain consortia can be used to design three- and four-strain ecosystems with predictable behaviors, and further extended to provide insights into community dynamics in space. This work sheds light on the organization of interacting microbial species, and provides a systematic framework—social interaction programming—to guide the development of synthetic ecosystems for diverse purposes.

Introduction

Designer microbial consortia are communities of rationally designed, interacting microorganisms that are capable of producing desired behaviors[1-4]. In the past decade, an array of such synthetic systems were developed, enabling different applications such as generating specific ecological dynamics[5-9], promoting species growth[10,11] and synthesizing valuable chemicals[12,13]. Compared to engineered isogenic populations, synthetic communities offer an increased degree of robustness for designed cellular functions and an expanded spectrum of functional programmability for complex tasks, thereby enabling novel and versatile biotechnological applications in complex settings[1]. Synthetic microbial consortia have also emerged as a promising engineering tool to manipulate microbiomes, such as those in the human body and in the rhizosphere, which helps to realize the enormous potential of microbiomes for therapeutic, environmental, and agricultural purposes[14-17]. However, despite increasing exciting proof-of-concept demonstrations, the utilization of such synthetic ecosystems is hampered by our limited ability in rapidly developing microbial ecosystems with desired temporal and spatial dynamics.

Cellular social interactions, such as competition and cooperation, are ubiquitous in microbial communities and shown to be essential in specifying ecosystem dynamics[18]. For instance, engineering cross feeding offers species co-existence[10,19,20] while building predator-prey interactions can lead to oscillatory, bistable or mono-stable behaviors[6]. Inspired by these findings, here we present a systematic framework to the design, construction and characterization of synthetic microbial communities, namely, social

interaction programming that combines modular pathway reconfiguration with model creation. Specifically, we employed a modular pathway reconfiguration approach to create six distinct consortia whose dynamics is specified by their underlying interaction modes. Using a modular approach similar to our experimental construction, we also derived quantitative models that captured experimentally observed population patterns. We further showed that the models from two-strain consortia can be used to design and build three- and four-strain ecosystems with predictable behaviors, and extended our investigations to yield insights into spatial community dynamics. Together, we established social interaction engineering as an effective and valuable route for ecosystem programming.

Results

Modular pathway reconfiguration for programing social interactions

Synthetic gene circuits are typically constructed from the bottom up by assembling individual DNA parts[21-26]; in principle, they can also be created through modular reconfiguration of existing gene clusters (Fig. 1a). Although having been barely practiced, modular cluster reconfiguration can be powerful for rapid circuit engineering due to the increasing complexity of desired functionalities[27] and the high modularity of native gene networks[28]. Inspired by this concept, we harnessed the modular biosynthesis pathways of nisin and lactococcin A (lcnA) in *Lactococcus lactis* (Fig. 1b) to develop programmable cells that could form the basis for synthetic microbial consortia. Of note, nisin, an antimicrobial and quorum-sensing molecule, is encoded by an eleven-gene cluster involving five functional modules, including precursor production,

translocation and initial modification, secondary modification, immunity and signaling[29] (Fig. 1c); and lcnA is an antimicrobial peptide whose underlying pathway consists of precursor production, translocation and immunity modules[30] (Fig. 1d).

The functional modularity of the pathways allowed us to rapidly generate different social interactions by selecting and tuning the molecules' signaling and bactericidal features through the alteration of module combinations. Specifically, we were able to create six synthetic microbial consortia that collectively enumerate all possible modes of pairwise social interactions[18,31-33] (Fig. 1e).

Engineering consortia with unidirectional interactions

We started by constructing a two-strain consortium of commensalism within which one benefits the other. Using our previously developed synthetic biology platform[34,35], we generated one strain (CmA) by introducing into *L. lactis* (NZ9000) the full nisin pathway and the constitutively expressed tetracycline resistance gene (tet^R). We also created the other (CmB) by transforming into NZ9000 a reconfigured version of the nisin pathway, which contains only the signaling and immunity modules, and a nisin-inducible tet^R expression circuit (Fig. 2a and Supplementary Fig. 1). Here, CmA was designed to secrete nisin to trigger the expression of tet^R in CmB, thereby conferring tetracycline resistance on CmB. Additionally, we inserted constitutively expressed fluorescent protein genes, *gfpuv* and *mCherry*, into the strains for observation and analysis.

102 As anticipated, CmA grew by itself in the GM17 media containing tetracycline due to its
103 constitutive *tet*^{R} expression; in contrast, CmB by itself did not grow, as its resistance is
104 not autonomous (Fig. 2b). However, CmA and CmB both grew when co-cultured (1:1
105 ratio) (Fig. 2b), suggesting that the presence of CmA conferred a growth benefit to CmB.
106 Such behaviors were also observed in a variant of the consortium where the *tet*^{R}
107 expression of CmA is nisin-inducible (Supplementary Fig. 2a). Additional experiments
108 showed that CmB grew in the tetracycline-containing media when nisin is supplemented
109 (Supplementary Fig. 2b) but failed to grow when CmA's nisin production is abolished
110 (Supplementary Fig. 2c). Furthermore, we showed that CmB growth was not due to
111 tetracycline degradation or absorption by CmA (Supplementary Fig. 3). Together, these
112 results confirmed that the mechanism of commensalism is the tetracycline resistance of
113 CmB induced by nisin released from CmA. Notably, as CmA and CmB were constructed
114 from the same parental strain (NZ9000), they had an indirect nutrient competition during
115 co-culture, and CmA had a reduced saturation density compared to the case of
116 monoculture.
117
118 We next engineered a consortium of amensalism, where one strain adversely affects
119 the other, by leveraging the bactericidal nature of nisin. Specifically, we created one
120 strain (AmA) by transplanting into NZ9000 the full nisin pathway and the other strain
121 (AmB) by simply introducing the vector pCCAMβ1 (Fig. 2d and Supplementary Fig. 1).
122 Again, fluorescence protein genes (*gfpuv* and *mCherry*) were introduced as reporters.
123 We found that, individually, AmA and AmB both grew up to saturation in GM17 media;
124 however, when co-cultured, only AmA was able to grow (Fig. 2e), demonstrating the

existence of a deleterious effect from AmA on AmB. Mechanistically, this effect arose from AmA's production of nisin that inhibits the growth of AmB. Utilizing the bactericidal nature of lcnA, we also constructed another version of amensalism by loading the lcnA pathway to NZ9000 to create a new toxin producer (AmA2) (Supplementary Figs. 4a and 1). Subsequent culturing experiments (Supplementary Fig. 4b) confirmed that the new ecosystem indeed involves one-way deleterious interaction.

We further constructed a two-strain consortium of neutralism, as a control to commensalism and amensalism, by loading to NZ9000 the vector (pCCAMβ1) and reporters (*gfpuv* and *mCherry*) (Fig. 2g and Supplementary Fig. 1). The two resulting strains, NeA and NeB, were able to grow both individually and together (Fig. 2h), confirming that their social interaction is indeed neutral. Notably, the reduction of each strain's saturation density in co-culture was due to indirect nutrient competition.

To quantitatively describe the observed behaviors, we constructed a mathematical framework for two-strain community dynamics using ordinary differential equations (Online Methods and Supplementary Note 1). The framework involves five variables, including two for the strain populations, two for the interacting molecules produced by the strains, and one for the nutrient in culture (Supplementary Eq. S1). In concert with the modular configurability of the bacteriocin pathways for gene circuit development, this modeling framework allows modular alterations to describe specific types of ecosystems. Upon data fitting, four derived models (Supplementary Note 4) successfully captured the population-dynamics characteristics of the consortia of

148 commensalism (Fig. 2c), amensalism (Fig. 2f and Supplementary Fig. 4c) and
149 neutralism (Fig. 2i).
150
151 **Developing consortia with bidirectional interactions**
152 Leveraging the modularity of the nisin and lcnA pathways, we next created consortia
153 involving two-way social interactions, namely cooperation, competition and predation.
154 Cooperation is the process where multiple species work together to accomplish a task
155 that yields mutual benefit. To create such a consortium, we designed the common task
156 as nisin production, a multi-step process including precursor production, translocation
157 and post-translational modification (Fig. 1c). The task was divided by assigning one
158 strain (CoA) to synthesize and secrete nisin precursor and the other (CoB) to convert
159 the precursor in the extracellular milieu into active nisin. Tetracycline resistance was
160 chosen as the benefit for completing the task. We developed these two strains by
161 modularly reconfiguring the nisin pathway and introducing nisin-inducible tet^R and
162 reporter systems (Fig. 3a and Supplementary Fig. 1).
163
164 Our growth experiments showed that CoA and CoB did not grow in tetracycline-
165 supplemented GM17 media unless they were co-cultured (Fig. 3b). For comparison,
166 each of the strains was able to grow when the media was supplemented with nisin
167 (Supplementary Fig. 5a). Additionally, abolishing the function of either strain (e.g.,
168 precursor translocation by CoA and modification by CoB) resulted in no growth of either
169 strain (Supplementary Fig. 5b, c). These results demonstrated the necessity of
170 cooperation for the growth of the engineered strains.

171

172 Competition is an interaction between species in which the fitness of one is lowered by
173 the presence of another. We designed an ecosystem with such an interaction by
174 utilizing the antimicrobial features of nisin and lcnA. Experimentally, we generated two
175 competing strains, named CpA and CpB, by introducing the nisin and lcnA pathways
176 into NZ9000 separately (Fig. 3d and Supplementary Fig. 1). Notably, CpA and CpB are
177 essentially the same as AmA and AmA2 (the two versions of toxin producers for
178 amensalism), because competition is the superposition of two counter-oriented,
179 detrimental interactions. We found that CpA and CpB both followed a logistic growth
180 pattern individually but, when co-cultured, CpA grew with a significant time delay (12
181 hrs) and CpB failed to grow (Fig. 3e) indicating that the fitness of the both strains was
182 reduced with their mutual presence. In this case, CpA won the competition and
183 dominated the population. Notably, although CpB lost the contest, lcnA it released at the
184 beginning of the experiment caused the growth delay and reduction of CpA in co-culture.
185

186 It has been theoretically predicted that differential outcomes may arise in competition by
187 altering ecosystem parameters such as relative interaction strengths[36]. To test these
188 predictions, we generated multiple variants of CpA and CpB by tuning their bacteriocin
189 productivities, including CpA2 (a lowered translation initiation rate (TIR) of nisB), CpB2
190 (a wild-type TIR of lcnA) and CpB3 (an increased TIR of lcnA) (Supplementary Tables 1
191 and 2). Using different combinations of the variants, we indeed observed distinct
192 competition outcomes including CpB dominance (Supplementary Fig. 6a) and close
193 contests (Supplementary Fig. 6b, c).

Predation is a social interaction where one species (prey) benefits another (predator) while being harmed. It is topologically equivalent to the combination of two unidirectional interactions, commensalism and amensalism, with opposite orientations. In light of this equivalence, we established a community of predation by assigning CmA of commensalism, a nisin producer with constitutive tetracycline resistance, as prey (PrA) and combining the circuits of CmB (nisin-inducible tet^R) and AmA2 (constitutive lcnA production) to form a predator (PrB) (Fig. 3g and Supplementary Fig. 1). In this design, PrA provides the benefit of tetracycline resistance to PrB by secreting nisin, while PrB hurts PrA through the release of lcnA.

When the resulting strains were co-cultured, PrA grew in the first 8 hours but gradually declined to a steady density afterwards, while PrB grew poorly at the beginning but faster later and eventually dominated the population, opposite to the monoculture where PrA grew normally but PrB failed to grow (Fig. 3h). The results confirmed the presence of the predatory relation between PrA and PrB, with the former serving as the prey and the latter as the predator. A variant of the ecosystem with similar behaviors involves the replacement of constitutive tetracycline resistance in PrA with nisin inducibility (Supplementary Fig. 7a). In addition, we confirmed that, in this relationship, both the beneficial and deleterious interactions are mandatory, through the monoculture experiments with nisin supplementation (Supplementary Fig. 7b) and the co-culture experiments where PrA or PrB was replaced by a neutral strain (Supplementary Fig. 7c, d)

To achieve a quantitative understanding of the above two-way ecosystems, we reconfigured our mathematical framework to create three ecosystem models (Supplementary Note 1). Consistent with the experiments, these models were able to generate distinct community dynamics for the cases of cooperation (Fig. 3c), competition (Fig. 3f and Supplementary Fig. 6d-f) and predation (Fig. 3i). Together, the mathematical modeling and experimental development of synthetic ecosystems demonstrated that social interaction engineering is a versatile and effective way to create desired two-strain microbial consortia.

Model-guided design of three- and four-strain ecosystems

To further illustrate the utility of our engineering method, we applied it to tackle a key challenge in microbiome and synthetic ecosystem research, namely, to design complex ecosystems with predictable dynamics. Specifically, we combined our established experimental consortia with mathematical models to determine if the dynamics of complex communities (e.g., three- and four-strain ecosystems) could be predicted from the behaviors of simple two-strain ecosystems. Using the models extended modularly from the two-strain cases (Supplementary Note 2), we first predicted the dynamic behaviors of eight three-strain microbial ecosystems formed by introducing third strains into the existing two-strain consortia. Importantly, in the process of model extension and dynamics prediction, all of the parameters from the two-strain communities remained fixed. The only new parameters were the growth rates of the newly introduced strains (i.e., the third strains), which had not been previously characterized.

240

241 To test the model predictions, we experimentally constructed eight third strains (CoAg,
242 CoBg, CpAg, CpBg, CmAg, CmBg, AmAg, and AmBg) in alignment with our models
243 (Online Methods; Supplementary Table 1; Supplementary Note 2). These third strains
244 were derived from the corresponding parent strains in the two-strain consortia (CoA,
245 CoB, CpA, CpB, CmA, CmB, AmA, and AmB) by using a colorimetric reporter gene
246 (*gusA*) to substitute the fluorescence reporter genes (*gfpuv* or *mCherry*). Therefore, the
247 third strains have identical interaction modes as their ancestors, but different growth
248 rates due to the alteration of their reporter systems. For instance, CoAg has the same
249 cooperation features as CoA but a different growth.

250

251 After measuring the growth rates of the third strains, we mixed them with the two-strain
252 consortia to form the eight three-strain communities, and performed ecosystem culture
253 experiments (Online Methods). Figure 4 shows the comparison of the model predictions
254 (lines) and experimental measurements (circles) of the eight three-strain ecosystems,
255 which demonstrates that the models successfully predicted the dynamics of the
256 synthetic communities. Notably, the dynamics of these communities can be explained
257 by analyzing their social interaction networks. For instance, in the AmA-AmB-CpAg
258 consortium (Fig. 4c), AmA and CpAg both grew but AmB went extinct because AmA
259 and CpAg both produced nisin that suppressed AmB; in contrast, in the AmA-AmB-
260 CpBg consortium (Fig. 4d), all strains went extinct due to the fact that AmA produced
261 nisin inhibiting both CpBg and AmB and CpBg produced lcnA that suppressed AmA and
262 AmB.

We further tested the feasibility of predicting complex community behaviors from the knowledge of two-strain consortia in selected four-strain ecosystems. Similar to the three-strain cases, we extended the modeling framework to describe four four-strain communities formed through combinatorial strain mixing (Supplementary Note 2). Again, the only new parameters in the models were the growth rates of the newly introduced strains. In parallel, we experimentally developed three new strains, PrBn, CmBn and AmBn, by removing the fluorescence reporter genes of the strains PrB, CmB and AmB, respectively (Online Methods and Supplementary Table 1). Using the new and previous strains, we generated four four-strain ecosystems, performed their co-culture experiments, and further compared the measured population dynamics with the model predictions (Fig. 5). These findings show that the models derived from the two-strain ecosystems successfully predicted the dynamics of more complex, four-strain ecosystems.

Although complex communities may involve higher-order interactions, the agreement between the model predictions and experimental measurements in Figs. 4 and 5 demonstrated that, at least for the ecosystems primarily containing pairwise interactions such as those tested, their community dynamics can be derived from the behaviors of simpler consortia. Additionally, these results affirmed that social interaction engineering is an effective approach to program complex synthetic communities with desired dynamics.

286 **Spatial dynamics of three symmetrical ecosystems**

287 In natural habitats, microbial communities such as the human gut microbiome and the
288 rhizosphere microbiome often extend across space where cellular interactions are
289 subject to the diffusion of interacting molecules[37]. This motivated us to examine whether
290 social interactions play a similar role in spatial settings by using the consortia with
291 symmetrical interactions—neutralism, cooperation and competition—as examples.
292 Using a computational model involving reaction-diffusion equations (Online Methods
293 and Supplementary Note 3), we simulated the development of spatial structures of the
294 three ecosystems whose initial cells were randomly seeded. Our results
295 (Supplementary Figs. 8a and 9a) showed that strains (NeA and NeB) formed random
296 patterns in neutralism with their detailed cell distributions subject to initial seeding,
297 relative abundance and growth rates; for the case of cooperation, the strains (CoA and
298 CoB) tended to be co-localized in space and the patterns developed better with close
299 initial ratios than biased; in competition, homogeneous patterns of a single strain (CpA
300 or CpB) emerged. Spatially averaged statistics of the initial and final populations in the
301 three cases (Supplementary Fig. 8b) further suggested that the ecosystem population
302 ratio drifts unidirectionally in neutralism, converges in cooperation, and diverges in
303 competition.

304

305 To test these model predictions, we performed a series of spatial patterning
306 experiments using droplets of well-mixed consortia with varied strain ratios (90:1 to
307 1:90) but a fixed total density (OD_{600}=0.2) (Online Methods). Consistent with the
308 modeling predictions, the strains within individual colonies were randomly distributed

309 when neutral, co-localized in cooperation, and mutually excluded in competition (Fig. 6a
310 and Supplementary Fig. 9b). For comparison, we also examined the spatiotemporal
311 dynamics of the predation consortium, which showed an initial ratio-dependent pattern
312 that is distinct from the symmetrical cases (Supplementary Fig. 10).
313
314 For the case of cooperation, spatial patterns were better developed with close initial
315 ratios than with unbalanced ratios. However, we also noticed that CpB (red) in the
316 competing consortium dominated in the spatial structures at the 1:1 ratio, contradicting
317 the culture experiment where CpA (green) won the contest (Fig. 3e). We speculated
318 that the discrepancy arose from the different diffusibilities of nisin and lcnA caused by
319 the stronger hydrophobicity of the former, which was confirmed by the patterning
320 experiments on agar plates supplemented with Tween 20, a surfactant promoting nisin
321 diffusion (Supplementary Fig. 11a). For the same reason, the initial ratio separatrices of
322 the other three competing ecosystems all shifted towards a higher nisin producer
323 abundance (Supplementary Fig. 11b, c).
324
325 We further compared the relative abundances of the three symmetric consortia during
326 pattern developments. Similar to the modeling analysis, the experimental results (Fig.
327 6b) showed that the NeA fraction of the neutral consortium increased over time for all
328 initial conditions, the CoA fraction of the cooperative consortium converged towards
329 91% (i.e., 10:1 ratio), and the CpA fraction of the competitive consortium diverged
330 (either 100% or 0%) with the transition occurring between 3:1 and 1:1. For comparison,
331 population ratio changes in additional cases of competition were also calculated

(Supplementary Fig. 11d-g). To quantify our findings, we further computed the entropy, a measure of the diversity of an ecosystem, and the intensity correlation quotient (ICQ), a measure of strain co-localization in space, of the experimentally observed (Fig. 6c) and simulated patterns (Supplementary Fig. 11h, i). These results pointed to the existence of opposite population driving forces exerted by cooperation that promotes coexistence and by competition favoring mutual exclusion.

In addition to well-mixed colonies, we investigated community organization in structured environments where droplets of individual strains are spaced with varying distances (Supplementary Fig. 12a-c and Online Methods). For neutralism, we found that the strains (NeA and NeB) always coexisted. For cooperation, the strains (CoA and CoB) coexisted but their patterns decayed with the spacing from the well-mixed filled circles (0 mm), to back-to-back domes (3 mm) and to diminishing edges (5 mm). For competition, emerged patterns shifted from one-strain exclusive circles (0mm) to repelled two-strain domes (3 mm) and to full circles (5 mm) with the increase of droplet distance. For comparison, additional cases of competition were also experimentally tested (Supplementary Fig. 12d-g). The results confirmed that social interactions continue to serve as a driving force in structured settings; meanwhile, spatial factors, such as colony spacing in this case, function as additional regulators that modulate pattern emergence.

Discussion

With increasing appreciation of microbiomes' profound impacts on human health, environment and agriculture, understanding and manipulating complex microbial ecosystems has become a defining mission for microbiome science. Our study provides fundamental insights into the structure, dynamics and ecology of interacting microbial species by characterizing synthetic consortia that serve as well-defined abstractions of native communities. In addition, our work demonstrates that social interaction engineering, through the combination of modular pathway reconfiguration and model creation, is a systematic strategy to design ecosystem behaviors. Such a synthetic biology approach sets the stage for creating complex, community functions for a variety of applications. For example, toward microbial cell factories, social interaction programming can be utilized to build the population stability of multiple synthetic strains co-involved in the division of labor in chemical synthesis by introducing cross feeding or differentiating substrate utilizations; such augmented stability will boost the robustness and yield of chemical production during microbial fermentation. Social interaction engineering also enables to establish synthetic ecosystems with predictable temporal and spatial dynamics, which can serve as a controllable tool to systematically perturb microbiomes and further alter their structure and dynamics in a desired manner. Looking forward, as microbes inhabit primarily complex, natural environments, our engineering strategy will become more versatile by validating the translatability of its applications from well-controlled, laboratory conditions to realistic settings.

Methods

Methods, including statements of data availability and any associated accession codes and references, are available in the online version of the paper.

Acknowledgements

We thank M. Sivaguru, G. Fried and A. Cyphersmith for their help with colony imaging at the IGB Core Facilities at UIUC, and B. Pilas of the Roy J. Carver Biotechnology Center at UIUC for assistance with flow cytometry analysis in this study. We also thank H. Liu, W. van der Donk, X. Yang and A. Blanchard for stimulating discussions and help. This work was supported by the National Science Foundation (1553649, 1227034), the Office of Naval Research (N000141612525), the American Heart Association (12SDG12090025), the Center for Advanced Study at UIUC, National Center for Supercomputing Applications, the Paul G. Allen Frontiers Group, and the Defense Threat Reduction Agency (HDTRA1-14-1-0006).

Author Contributions

T.L. and J.J.C. designed the study; T.L. conceived the project; W.K. performed the experiments and collected the data; D.R.M. and T.L. developed the computational models; W.K., D.R.M. and T.L. analyzed the data; T.L., J.J.C., W.K. and D.R.M. discussed the results and wrote the paper.

Competing financial interests

The authors declare no competing financial interests.

399 **References**

400 1. Brenner, K., You, L. & Arnold, F.H. Engineering microbial consortia: a new
401 frontier in synthetic biology. *Trends Biotechnol.* **26**, 483-489 (2008).
402 2. Großkopf, T. & Soyer, O.S. Synthetic microbial communities. *Curr. Opin.*
403 *Microbiol.* **18**, 72-77 (2014).
404 3. De Roy, K., Marzorati, M., Van den Abbeele, P., Van de Wiele, T. & Boon, N.
405 Synthetic microbial ecosystems: an exciting tool to understand and apply
406 microbial communities. *Environ. microbiol.* **16**, 1472-1481 (2014).
407 4. Bittihn, P., Din, M.O., Tsimring, L.S. & Hasty, J. Rational engineering of synthetic
408 microbial systems: from single cells to consortia. *Curr. Opin. Microbiol.* **45**, 92-99
409 (2018).
410 5. Weber, W., Daoud-El Baba, M. & Fussenegger, M. Synthetic ecosystems based
411 on airborne inter-and intrakingdom communication. *Proc. Natl. Acad. Sci. USA*
412 **104**, 10435-10440 (2007).
413 6. Balagaddé, F.K. et al. A synthetic *Escherichia coli* predator–prey ecosystem. *Mol.*
414 *Syst. Biol.* **4**, 187 (2008).
415 7. Chen, Y., Kim, J.K., Hirning, A.J., Josić, K. & Bennett, M.R. Emergent genetic
416 oscillations in a synthetic microbial consortium. *Science* **349**, 986-989 (2015).
417 8. Gore, J., Youk, H. & Van Oudenaarden, A. Snowdrift game dynamics and
418 facultative cheating in yeast. *Nature* **459**, 253 (2009).
419 9. Chuang, J.S., Rivoire, O. & Leibler, S. Simpson's paradox in a synthetic microbial
420 system. *Science* **323**, 272-275 (2009).

421 10. Mee, M.T., Collins, J.J., Church, G.M. & Wang, H.H. Syntrophic exchange in
422 synthetic microbial communities. *Proc. Natl. Acad. Sci. USA* **111**, E2149-E2156
423 (2014).
424 11. Wintermute, E.H. & Silver, P.A. Emergent cooperation in microbial metabolism.
425 *Mol. Syst. Biol.* **6**, 407 (2010).
426 12. Zhou, K., Qiao, K., Edgar, S. & Stephanopoulos, G. Distributing a metabolic
427 pathway among a microbial consortium enhances production of natural products.
428 *Nat. Biotechnol.* **33**, 377-383 (2015).
429 13. Minty, J.J. et al. Design and characterization of synthetic fungal-bacterial
430 consortia for direct production of isobutanol from cellulosic biomass. *Proc. Natl.*
431 *Acad. Sci. USA* **110**, 14592-14597 (2013).
432 14. Hood, L. Tackling the microbiome. *Science* **336**, 1209-1209 (2012).
433 15. Cho, I. & Blaser, M.J. The human microbiome: at the interface of health and
434 disease. *Nat. Rev. Genet.* **13**, 260-270 (2012).
435 16. Falkowski, P.G., Fenchel, T. & Delong, E.F. The microbial engines that drive
436 Earth's biogeochemical cycles. *Science* **320**, 1034-1039 (2008).
437 17. Berendsen, R.L., Pieterse, C.M. & Bakker, P.A. The rhizosphere microbiome and
438 plant health. *Trends Plant Sci.* **17**, 478-486 (2012).
439 18. Faust, K. & Raes, J. Microbial interactions: from networks to models. *Nat. Rev.*
440 *Microbiol.* **10**, 538-550 (2012).
441 19. Shou, W., Ram, S. & Vilar, J.M. Synthetic cooperation in engineered yeast
442 populations. *Proc. Natl. Acad. Sci. USA* **104**, 1877-1882 (2007).

443 20. Brenner, K., Karig, D.K., Weiss, R. & Arnold, F.H. Engineered bidirectional
444 communication mediates a consensus in a microbial biofilm consortium. *Proc.*
445 *Natl. Acad. Sci. USA* **104**, 17300-17304 (2007).
446 21. Hasty, J., McMillen, D. & Collins, J.J. Engineered gene circuits. *Nature* **420**, 224-
447 230 (2002).
448 22. Endy, D. Foundations for engineering biology. *Nature* **438**, 449-453 (2005).
449 23. Andrianantoandro, E., Basu, S., Karig, D.K. & Weiss, R. Synthetic biology: new
450 engineering rules for an emerging discipline. *Mol. Syst. Biol.* **2**, 2006.2008 (2006).
451 24. Arkin, A. Setting the standard in synthetic biology. *Nat. Biotechnol.* **26**, 771-773
452 (2008).
453 25. Brophy, J.A. & Voigt, C.A. Principles of genetic circuit design. *Nat. Methods* **11**,
454 508-520 (2014).
455 26. Collins, J.J. et al. Synthetic biology: How best to build a cell. *Nature* **509**, 155-157
456 (2014).
457 27. Purnick, P.E. & Weiss, R. The second wave of synthetic biology: from modules to
458 systems. *Nat. Rev. Mol. Cell Biol.* **10**, 410-422 (2009).
459 28. Hartwell, L.H., Hopfield, J.J., Leibler, S. & Murray, A.W. From molecular to
460 modular cell biology. *Nature* **402**, C47-C52 (1999).
461 29. Lubelski, J., Rink, R., Khusainov, R., Moll, G. & Kuipers, O. Biosynthesis,
462 immunity, regulation, mode of action and engineering of the model lantibiotic
463 nisin. *Cell. Mol. Life Sci.* **65**, 455-476 (2008).

464 30. Stoddard, G.W., Petzel, J.P., Van Belkum, M., Kok, J. & McKay, L.L. Molecular
465 analyses of the lactococcin A gene cluster from *Lactococcus lactis* subsp. *lactis*
466 biovar diacetylactis WM4. *Appl. Environ. Microbiol.* **58**, 1952-1961 (1992).
467 31. West, S.A., Diggle, S.P., Buckling, A., Gardner, A. & Griffin, A.S. The social lives
468 of microbes. *Annu. Rev. Ecol. Evol. Syst.* **38**, 53-77 (2007).
469 32. Foster, K.R. Social behaviour in microorganisms. in *Social Behaviour: Genes,*
470 *Ecology and Evolution* 331-356 (Cambridge Univ. Press, Cambridge, 2010).
471 33. Xavier, J.B. Social interaction in synthetic and natural microbial communities. *Mol.*
472 *Syst. Biol.* **7**, 483 (2011).
473 34. Kong, W., Kapuganti, V.S. & Lu, T. A gene network engineering platform for
474 lactic acid bacteria. *Nucleic Acids Res.* **44**, e37 (2016).
475 35. Kong, W. & Lu, T. Cloning and optimization of a nisin biosynthesis pathway for
476 bacteriocin harvest. *ACS Synth. Biol.* **3**, 439-445 (2014).
477 36. Volterra, V. Variations and fluctuations of the number of individuals in animal
478 species living together. *ICES J. Mar. Sci.* **3**, 3-51 (1928).
479 37. Nadell, C.D., Drescher, K. & Foster, K.R. Spatial structure, cooperation and
480 competition in biofilms. *Nat. Rev. Microbiol.* **14**, 589-600 (2016).
481

Figures and Captions

Figure 1

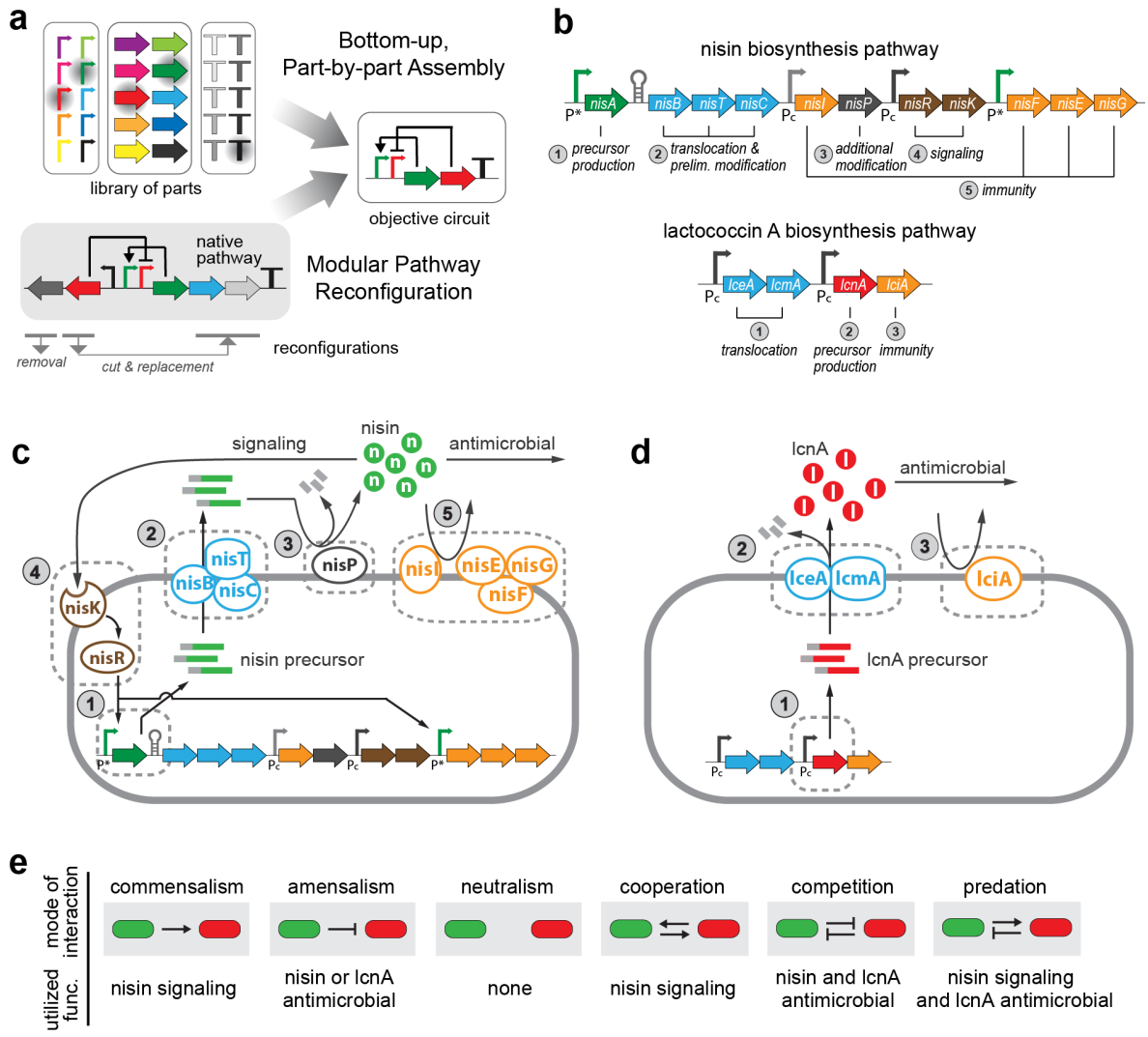

Figure 1: Modular pathway reconfiguration for engineering microbial consortia. (**a**) Two approaches to engineering gene circuits. A circuit can be created by assembling selected genetic parts from scratch or through modular reconfiguration of existing gene clusters. (**b**) nisin and lactococcin A (lcnA) biosynthesis gene clusters. (**c**) Modular organization of the nisin pathway. It involves five functionally independent modules, including those for precursor production (1), translocation and initial modification (2), additional modification (3), signaling (4), and nisin immunity (5). (**d**) Modular organization of the lcnA pathway. It contains three functionally independent

493 modules, including those for precursor production (1), translocation (2), and lcnA
494 immunity (3). (**e**) Design of six two-strain consortia that differentially utilize the signaling
495 and antimicrobial features of the bacteriocins.

Figure 2

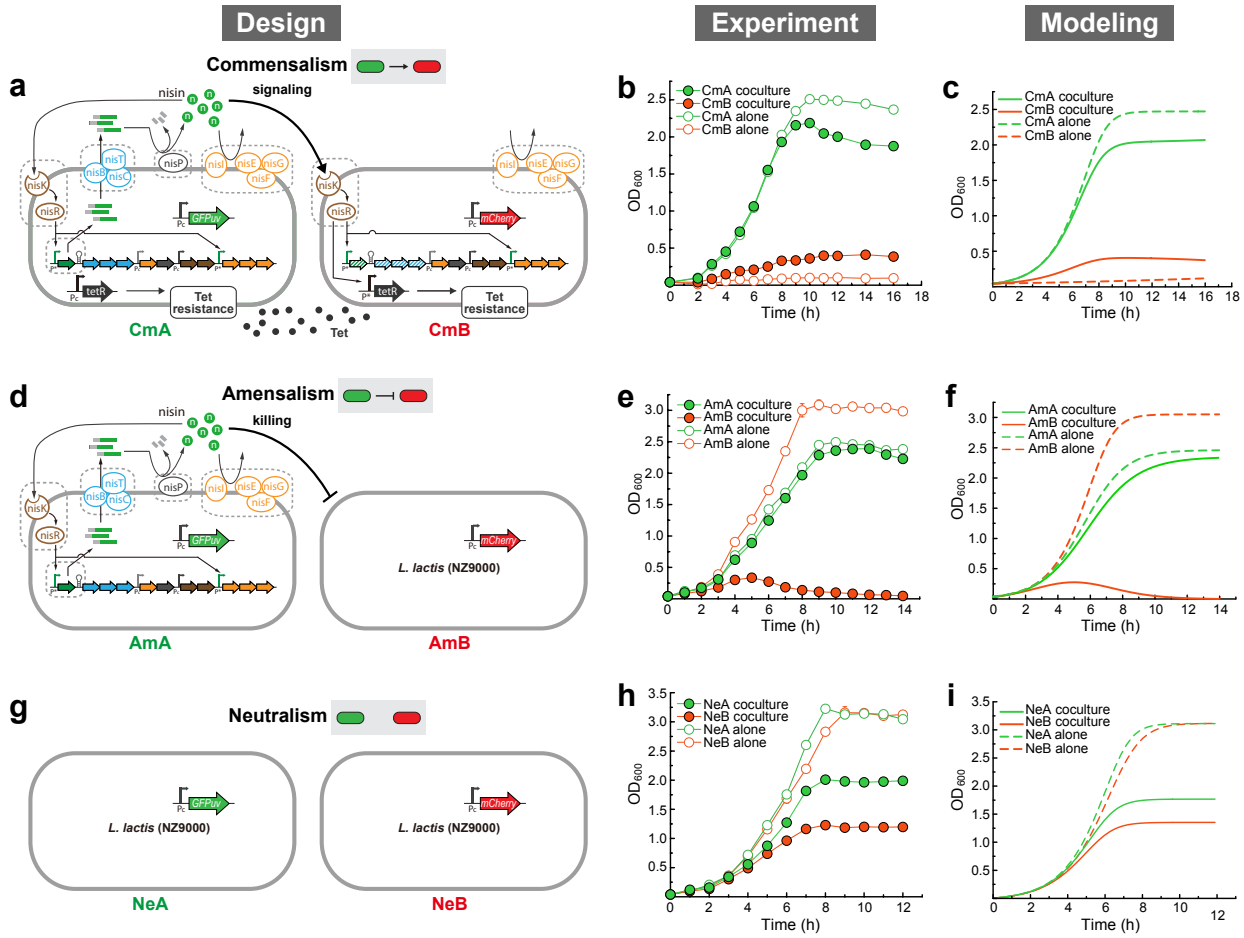

Figure 2: Synthetic consortia with one-way social interactions.
(**a**) Circuit diagram of a commensal microbial consortium. CmA is a nisin producer with constant tetracycline resistance. CmB has nisin-inducible tetracycline resistance. Here, genes filled with diagonal lines are knocked out. (**b**) Growth of CmA and CmB of the commensal consortium, in monoculture and co-culture experiments using GM17 media supplemented with tetracycline. (**c**) Simulated population dynamics for the commensal consortium. (**d**) Circuit diagram of a consortium of amensalism. AmA is a nisin producer that inhibits the growth of AmB. (**e**) Growth of AmA and AmB of the amensal consortium, in monoculture and co-culture experiments. (**f**) Simulated population dynamics for the consortium of amensalism. (**g**) Circuit diagram of a neutral consortium, where the two strains NeA and NeB do not have any active social interactions. (**h**) Growth of two neutral strains, NeA and NeB, in monoculture and co-culture experiments. (**i**) Simulated

population dynamics for the neutral consortium. In panels **b**, **e**, and **h**, closed and open circles stand for population growth in co- and monoculture experiments, respectively. In each co-culture experiment, strains were inoculated at 1:1 initial ratio. Experimental data are presented as mean (s.d.), n=3. In panels **c**, **f**, and **i**, dashed lines correspond to monoculture growth, while solid lines correspond to co-culture growth.

Figure 3

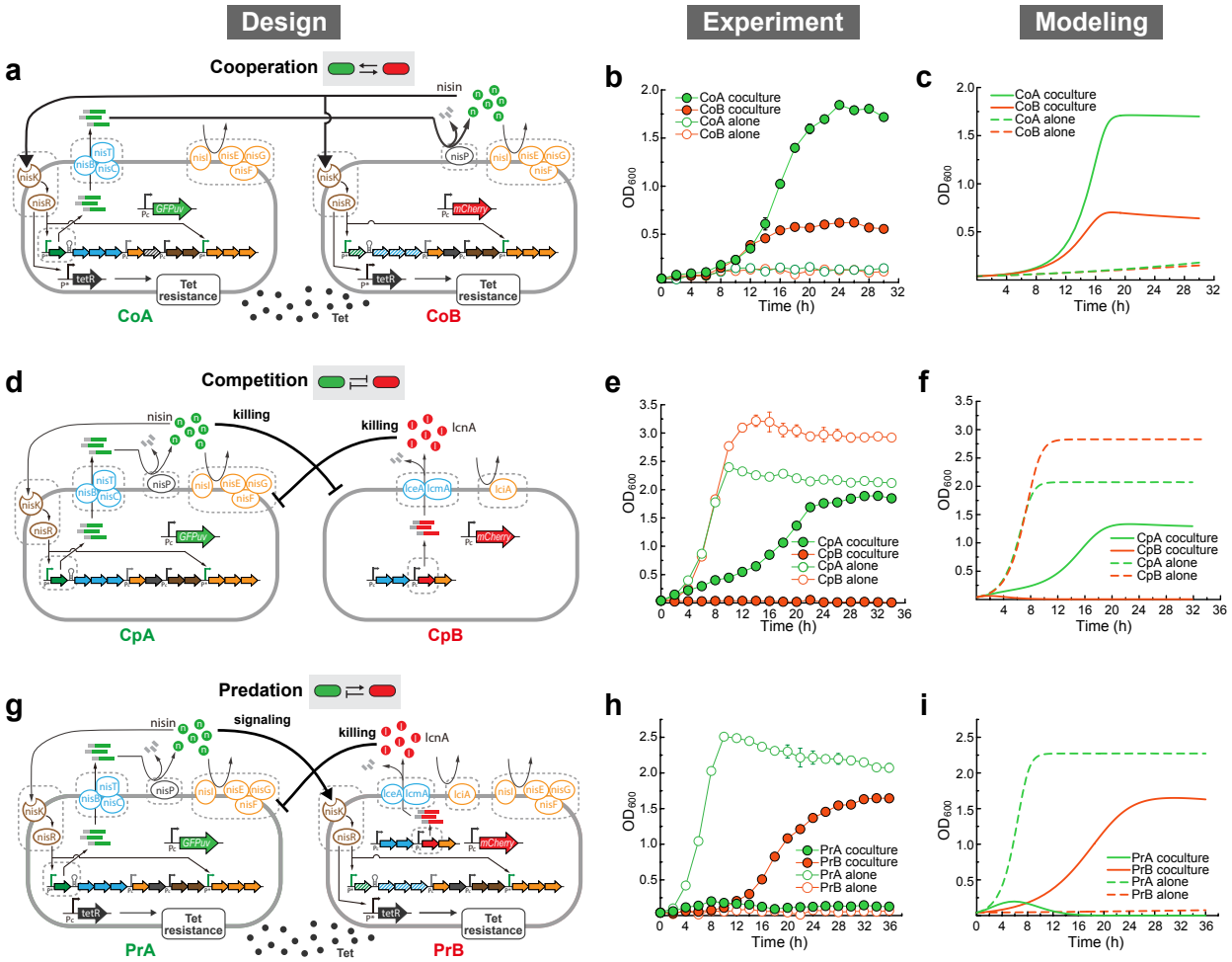

Figure 3: Synthetic consortia involving two-way social interactions. (**a**) Circuit diagram of a cooperative consortium. CoA produces nisin precursor and CoB modifies the precursor to produce active nisin, forming a cooperation of successful nisin production. Nisin induces the tetracycline resistance of both strains, which enables them to survive in tetracycline-supplemented media. Here, genes filled with diagonal lines are knocked out. (**b**) Growth of two cooperative strains (CoA and CoB) in co-culture and monoculture experiments. (**c**) Simulated population dynamics for the cooperative consortium. (**d**) Circuit diagram of a mutually competitive consortium. CpA is a nisin producer and CpB is a IcnA producer. CpA outcompetes CpB in the co-culture experiment. (**e**) Growth of two competitive strains (CpA and CpB) in co-culture and monoculture experiments. (**f**) Simulated population dynamics for the competing

consortium. (**g**) Circuit diagram of a predative consortium. PrA (prey) is a nisin producer with constant tetracycline resistance. PrB (predator) is an lcnA producer with nisin-inducible tetracycline resistance. PrA induces the growth of PrB by secreting nisin; in turn, PrB suppresses the growth of PrA by releasing lcnA. Here, genes filled with diagonal lines are knocked out. (**h**) Growth of two predation strains, PrA and PrB, in co-culture and monoculture experiments. (**i**) Simulated population dynamics for the consortium of predation. In panels **b**, **e**, and **h**, closed and open circles stand for population growth in co-culture and monoculture experiments, respectively. In each co-culture experiment, strains were inoculated at 1:1 initial ratio. Experimental data are presented as mean (s.d.), n=3. In panels **c**, **f**, and **i**, dashed lines correspond to monoculture growth, while solid lines correspond to co-culture growth.

Figure 4

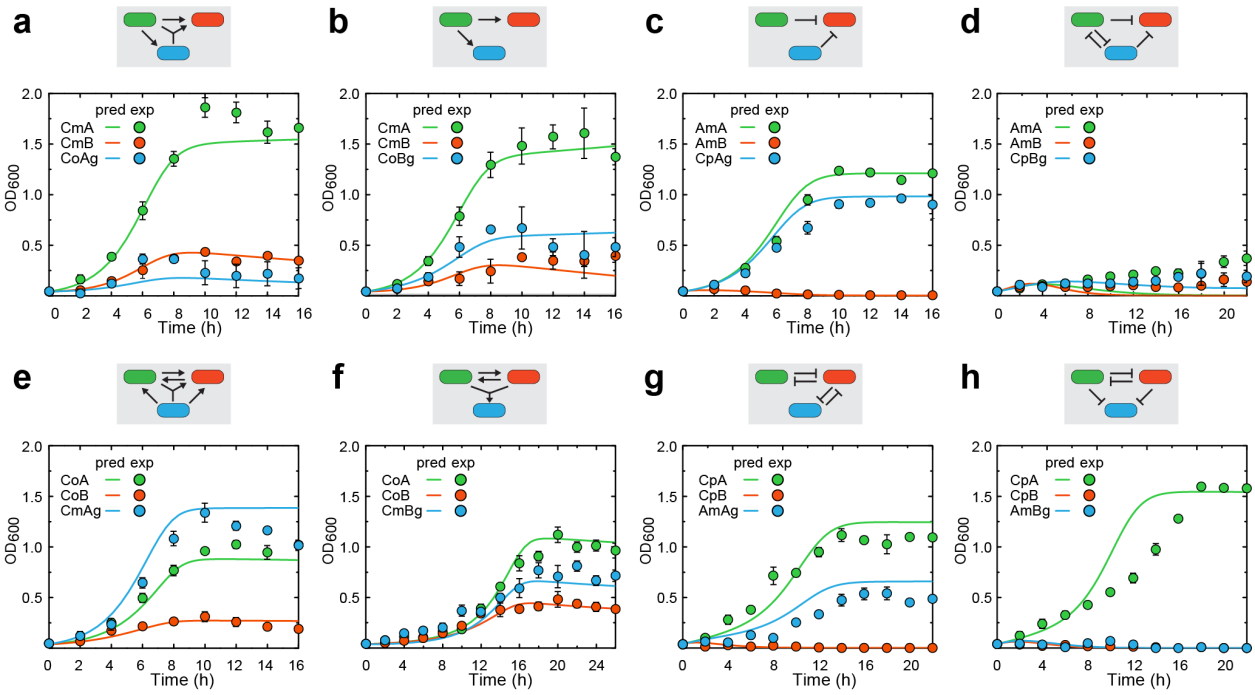

Figure 4: Model-predicted and experimentally measured population dynamics of three-strain ecosystems.

(**a**) Population dynamics of a three-strain consortium composed of the two commensalism strains (CmA and CmB) and a cooperation strain (CoAg). (**b**) Population dynamics of a three-strain consortium composed of the two commensalism strains (CmA and CmB) and a cooperation strain (CoBg). (**c**) Population dynamics of a three-strain consortium composed of the two amensalism strains (AmA and AmB) and a competition strain (CpAg). (**d**) Population dynamics of a three-strain consortium composed of the two amensalism strains (AmA and AmB) and a competition strain (CpBg). (**e**) Population dynamics of a three-strain consortium composed of the two cooperation strains (CoA and CoB) and a commensalism strain (CmAg). (**f**) Population dynamics of a three-strain consortium composed of the two cooperation strains (CoA and CoB) and a commensalism strain (CmBg). (**g**) Population dynamics of a three-strain consortium composed of the two competition strains (CpA and CpB) and an amensalism strain (AmAg). (**h**) Population dynamics of a three-strain consortium composed of the two competition strains (CpA and CpB) and an amensalism strain (AmBg). Each ecosystem's interaction network is shown on the top of the corresponding

559 panel. For all panels, lines and color circles stand for model predictions and
560 experimental results, respectively. Data are presented as mean (s.d.), n=3. In all co-
561 culture experiments, strains were inoculated at 1:1:1 initial ratio.
562

563 **Figure 5**

564

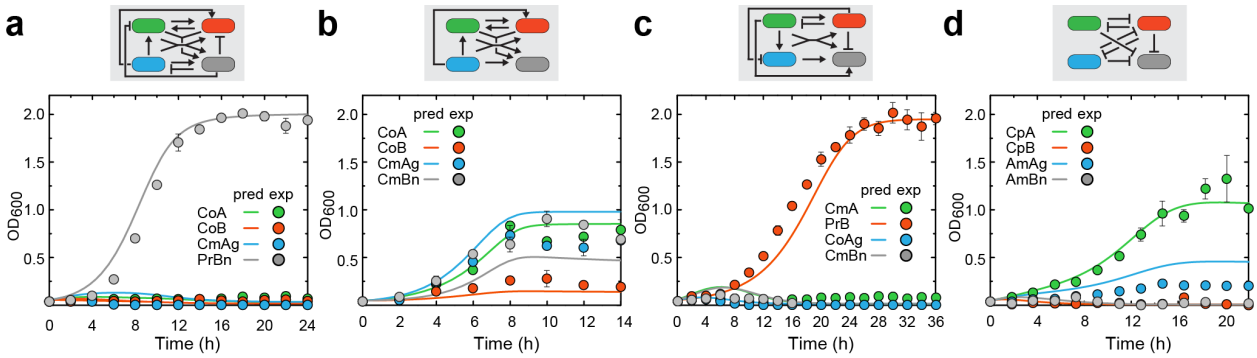

565

566 **Figure 5: Model-predicted and experimentally measured population dynamics of**
567 **four-strain ecosystems.**
568 (**a**) Population dynamics of a four-strain consortium composed of two cooperation
569 strains (CoA and CoB), a commensalism strain (CmAg) and a predation strain (PrBn).
570 (**b**) Population dynamics of a four-strain consortium composed of two cooperation
571 strains (CoA and CoB) and two commensalism strains (CmAg and CmBn). (**c**)
572 Population dynamics of a four-strain consortium composed of two commensalism
573 strains (CmA and CmBn), a predation strain (PrB) and a cooperation strain (CoAg). (**d**)
574 Population dynamics of a four-strain consortium composed of two competition strains
575 (CpA and CpB) and two amensalism strains (AmAg and AmBn). Each ecosystem's
576 interaction network is shown on the top of the corresponding panel. For all panels, lines
577 and color circles stand for model predictions and experimental results, respectively.
578 Data are presented as mean (s.d.), n=3. In all co-culture experiments, strains were
579 inoculated at 1:1:1:1 initial ratio.

580

Figure 6

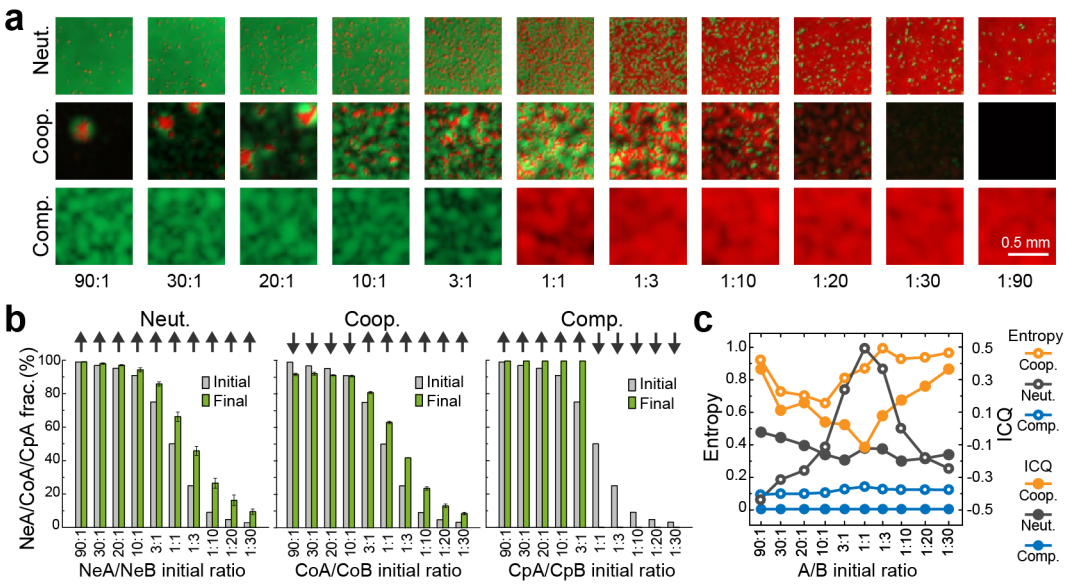

Figure 6: Spatial dynamics of three symmetrical communities.
(**a**) Spatial patterns emerged from the well-mixed consortia of neutralism, cooperation and competition growing on agar plates. A density of OD_{600}=0.2 and varied ratios from 90:1 to 1:90 were used as initial conditions. Each experiment was repeated at least three times. Representative pictures from the experiments are shown. (**b**) Comparison of the total initial and final population ratios of the consortia the experimental patterning processes. The NeA fraction increases in all cases due to a fast growth rate of NeA, the CoA fraction converged to ~90%, and CpA fraction diverged to either 100% or 0% depending on the initial conditions. Experimental data are presented as mean (s.d.), n=3. (**c**) Entropy (open circles) and intensity correlation quotient (ICQ) (closed circles) of the experimental patterns in panel **a**. The values of entropy and ICQ both follow the order of cooperation > neutralism > competition, although they are subject to initial conditions. Data are averaged from n=3 experiments. Each experiment was repeated at least three times. Representative pictures from experiments are shown.

601 **Online Methods**

602 **Strains.** *Lactococcus lactis* NZ9000 was used as host for strains in all ecosystems.
603 Lactococcal strains were cultured in M17 medium with 0.5% glucose (GM17) at 30°C. All
604 plasmids were first constructed and sequenced in *E. coli* NEB-10β, then transformed into *L.*
605 *lactis* by electroporation. Antibiotics were added as required: chloramphenicol (10 μg ml^{-1}),
606 erythromycin (250 μg ml^{-1}), tetracycline (3 μg ml^{-1}), kanamycin (50 μg ml^{-1}), spectinomycin
607 (50 μg ml^{-1}), and streptomycin (150 μg ml^{-1}) for *E. coli*, and chloramphenicol (5 μg ml^{-1}),
608 erythromycin (5 μg ml^{-1}), and tetracycline (10 μg ml^{-1}) for *L. lactis*. Please see
609 Supplementary Table 1 for full strain and plasmid information.

610

611 **Construction of the reporter and selector plasmids.** Oligos for plasmid construction are
612 listed in Supplementary Table 2. All reporter and selector plasmids were developed from an
613 *L. lactis-E. coli* shuttle vector, pleiss-Nuc, which contains a pSH71 origin, a chloramphenicol
614 resistance gene, a PnisA promoter from a nisin gene cluster, and a Nuc reporter[38]. Gibson
615 assembly was used to construct all the reporter and selector plasmids. The plasmid for
616 constitutively expressing GFP (pleiss-Pcon-gfp) was constructed by replacing PnisA
617 promoter and Nuc in pleiss-Nuc with a *gfpuv* gene and the constitutive promoter of *lcnA*[30].
618 The plasmid for constitutive expression of RFP, pleiss-Pcon-rfp, was constructed by
619 replacing *gfp* in pleiss-Pcon-gfp with *mcherry*. The selector plasmids pleiss-Pnis-tet-Pcon-
620 gfp and pleiss-Pnis-tet-Pcon-rfp were constructed by amplifying tet^R gene from the plasmid
621 pVPL3112 and Pcon-gfp or Pcon-rfp cassette from the plasmid constructed above and
622 cloning them into pleiss-Nuc[39]. The tet^R gene was under the control of PnisA promoter. The
623 plasmid pleiss-Pcon-tet-Pcon-gfp was constructed by insertion of tet^R and its RBS
624 downstream of *gfp* in pleiss-Pcon-gfp. Both *gfp* and tet^R were under the control of the
625 constitutive promoter of *lcnA*. The reporter and selector plasmids encoding a β–

626 glucuronidase (GusA)[40] were constructed by replacing *gfp* in the plasmids pleiss-Pnis-tet-
627 Pcon-gfp and pleiss-Pcon-tet-Pcon-gfp with *gusA*. The reporter-free selector plasmids were
628 constructed by deleting the *gfp* gene from pleiss-Pnis-tet-Pcon-gfp and pleiss-Pcon-tet-
629 Pcon-gfp.
630
631 **Construction of the plasmids for nisin production and nisin resistance.** All nisin-
632 producing plasmids in ecosystems were constructed based on the plasmid, pWK6, which
633 was cloned by insertion of a wild-type nisin gene cluster from *L. lactis* k29 into pCCAMβ1;
634 an *L. lactis*-*E. coli* shuttle vector[34,35]. To avoid leaky expression of promoter PnisA in cells
635 provided with multi-copy *nisRK*, the *nisRK* gene in the multi-copy plasmid pWK6 was
636 knocked out. In brief, the plasmids pWK6 and the Red/ET recombination plasmid pRedET
637 (GeneBridges) were transferred into NEB-10β to generate the strain NEB-
638 10β/pWK6/pRedET. Then the *aadA* gene (spectinomycin resistant gene) was amplified
639 from plasmid pBeta[34] and the generating fragment was flanked with a short sequence of 3'
640 of *nisP* and 5' of *nisF* and transformed into the induced competent cells of NEB-
641 10β/pWK6/pRedET using the protocol described previously[34]. After recombination, the
642 *nisRK* gene in pWK6 was replaced with the *aadA* gene, generating a new plasmid pWK6-
643 RK$^-$. Then, pWK6-RK$^-$ was transferred into *L. lactis* NZ9000 (a single copy *nisRK* in its
644 chromosome) to test the complementation and recovery of the nisin positive phenotype.
645 The plasmid pWK6 was also engineered to reduce its nisin productivity through
646 reducing the RBS strength of *nisB* using ssDNA recombination performed as described
647 previously[34]. In brief, a 90-nt ssDNA oligo nisB269 embracing an RBS sequence with a
648 translation initiation rate (TIR) of 269 AU was designed using RBS calculator
649 (https://salislab.net/software/). The ssDNA was transferred to the Beta protein expressing
650 NEB-10β::MutS/pBeta/pWK6 to replace the wild-type *nisB* RBS (TIR=104148 AU) through

651 ssDNA recombination, thus generating the plasmid pWK6b. The plasmid pWK6b was
652 further engineered to generate a *nisRK* knock-out version pWK6b-RK$^-$ according the
653 method described above. Then, pWK6b-RK$^-$ was also transferred to *L. lactis* NZ9000 to test
654 *nisRK* complementation.

655 The nisin resistant plasmid was developed based on pWK6. First, the start codon
656 and RBS of *nisA* were mutated in pWK6 by ssDNA recombination using a 90-nt oligo
657 nisAmut. Second, *nisP* and *nisRK* were knocked out by selection and counter-selection
658 using a knstrep cassette as described previously[34]. Briefly, knstrep cassette flanking with 5'
659 of *nisP* and 3' of *nisRK* was PCR amplified and transferred to NEB-10β/pWK6/pRedET
660 replacing *nisPRK*. A fragment generated by fusion of a short fragment of 5' of *nisP* and 3' of
661 *nisRK* using overlap extension PCR (OE-PCR) was transformed into the strain to replace
662 knstrep by counter selection. Third, nisBTC was knocked out using the same method. The
663 resulting plasmid was named pWK6-IFEG. Though pWK6-IFEG was unable to produce and
664 modify nisin, it has all promoters and nisin immunity genes; it was transferred to *L. lactis*
665 NZ9000 to test nisin immunity.

666

667 **Construction of the plasmids for nisP$^-$ nisin precursor producer and nisP$^+$ nisin**
668 **resistant strain.** The NisP deficient prenisin synthesis plasmid for cooperation was
669 constructed from the plasmid pWK6b. First, *nisP* and *nisRK* genes in pWK6b were knocked
670 out by replacing them with knstrep cassette. Second, a fragment combining 5' of *nisP* and 3'
671 of *nisRK* was generated by overlap extension PCR and used to replace the knstrep
672 cassette by counter selection. The resulting plasmid was named pWK6b-PRK$^-$. The NisP+
673 nisin resistant plasmid for cooperation was generated from pWK6. First, start codon and
674 RBS of *nisA* were mutated in pWK6 by ssDNA recombination using the 90-nt oligo nisAmut.
675 Second, *nisRK* were knocked out by selection and counter selection using the knstrep

676 cassette. Third, *nisBTC* was knocked out by selection and counter selection. The resulting
677 plasmid was named pWK6-IPFEG. Then, it was transferred to *L. lactis* NZ9000 to test nisin
678 immunity. In addition, NZ9000/ pWK6b-PRK$^-$ and NZ9000/ pWK6-IPFEG were co-cultured
679 at 1:1 ratio to examine their ability in cooperative production of nisin.
680
681 **Construction of the plasmid for lcnA producer.** Genes of lcnA gene cluster were
682 amplified from plasmid pFI2396 and pFI2148 and assembled with P32 promoter into pleiss-
683 Nuc vector in the following order: pleiss-3'-lciA-lcmA-lceA-Promoter-5'-5'-P32-lcnA-3'-pleiss
684 (P32-lcnA has a different direction with other genes in the cluster)[41]. The RBS TIR of the
685 precursor gene *lcnA* was changed by designing of RBS sequence with different TIR using
686 RBS calculator. Then the lcnA gene cluster was amplified and subcloned to *Not* I site of
687 pCCAMβ1 by Gibson assembly. Two variants pWK-lcnA^{5k} and pWK-lcnA^{20k} with TIR of
688 5078 AU and 19950 AU were chosen for subsequent experiments. In addition, genes of
689 lcnA gene cluster were also assembled to wild-type gene cluster with their native promoters
690 in original order in pleiss-Nuc vector. The wild-type gene cluster was then transferred to
691 pCCAMβ1 to generate the plasmid pWK-lcnA^{wt}.
692
693 **Construction of the plasmid with nisin resistance and lcnA gene cluster.** The plasmid
694 with both nisin resistance and lcnA production in predation was constructed by combining
695 pWK-lcnA^{wt} and pWK6. First, pWK6 was engineered to *nisA* mutation, *nisBTC* knockout and
696 *nisPRK* knockout by ssDNA recombination and selection and counter selection as
697 mentioned above. Then, the modified nisin gene cluster with only nisin resistance function
698 was amplified and cloned to *Not* I site of pWK-lcnA^{wt} through Gibson assembly. The
699 resulting plasmid was named pWK6-IFEG-lcnA^{wt}.
700

701 **Agar diffusion assay.** All the nisin producer plasmids were transformed into *L. lactis*
702 NZ9000. Agar diffusion assays were performed to measure nisin productivity of modified
703 nisin producers and cooperative strains in cooperation as well as lcnA productivity of lcnA
704 producers. Agar diffusion assay was performed as previously described[34] except a new *L.*
705 *lactis* 117 indicator strain was used. The plasmid pCCAMβ1 (Erm^R) and pleiss-Pcon-tet-
706 Pcon-gfp (Cm^R Tet^R) were co-transformed to *L. lactis* 117 so that it was resistant to
707 erythromycin, chloramphenicol and tetracycline simultaneously. Then, the inhibition zone
708 could affect the concentration of nisin in the culture without interference of antibiotics.
709
710 **Co-culture experiments.** Bacterial strains were grown overnight in GM17 media containing
711 chloramphenicol and erythromycin to an early stationary phase. Bacteria were centrifuged
712 and washed twice with fresh GM17 media. Then OD_{600} of the cells was adjusted to 2.0.
713 Each strain in co-culture or monoculture was inoculated to fresh media with appropriate
714 antibiotics at a 1:50 dilution. For neutralism, amensalism and competition, erythromycin and
715 chloramphenicol were added. For commensalism, cooperation and predation, erythromycin
716 and tetracycline were added for selection. Samples were taken from the cultures every two
717 hours for measurement of growth. Meanwhile, cells from 500 μl of cultures were centrifuged
718 and resuspended in PBS buffer. The cells were diluted to 10^6 cells ml^{-1} and stored in PBS
719 buffer at 4°C for at least 4 hours then vigorously vortexed breaking most chains of
720 lactococci into single cells. Then green and red fluorescent cells in the sample were
721 counted by a Flow cytometer (BD LSR Fortessa). GFP was measured on the FITC channel,
722 excited with a 488-nm blue laser and detected with a 530/30-nm bandpass filter. RFP was
723 measured on PE-Texas Red channel using a 561-nm yellow/green laser and a 610/20-nm
724 bandpass filter. At least 10,000 events were recorded for green and red cell counting per
725 sample. In addition, images with green and red fluorescence were also taken by a

726 fluorescence microscope and at least 1000 cells from each sample were counted manually.
727 The GusA-containing strains in the three- and four-strain consortia were distinguished by
728 their blue color on GM17 agar plates containing 50 μg ml^{-1} of X-gluc (5-Bromo-4-chloro-3-
729 indolyl beta-D-glucuronide sodium salt), and their colony forming units (CFUs) were counted
730 to calculate their ratio in the population. For the no-color strains in four-strain consortia, their
731 populations were obtained by subtracting the numbers of green, red and blue cells from the
732 total populations. The growth curve of each strain in the population was drawn by
733 multiplying total OD_{600} of the population with individual ratios. Control experiments with a
734 single strain in commensalism, cooperation and predation induced with nisin was performed
735 as follows: overnight cultures (diluted to OD_{600}=2.0) were inoculated to fresh GM17 media
736 with erythromycin, tetracycline and 25 ng ml^{-1} of nisin (1 IU=25 ng) at a ratio of 1:50. Then
737 the culture was incubated at 30°C and cell densities were measured at one or two hours'
738 intervals.
739
740 **Spatial patterns of well-mixed consortium droplets.** Overnight single-strain cultures for
741 neutralism, cooperation and competition were centrifuged and washed with fresh GM17
742 media. The cells were diluted to an OD_{600} of 0.2 using fresh media. Strain A and strain B in
743 each ecosystem were mixed at different ratios from 90:1 to 1:90. Then 1 μl of the mixture
744 was added onto a 90-mm agar plate (20 ml of GM17 agar with appropriate antibiotics and
745 2% agar). The plates were incubated at 30°C for different time. The incubation time was
746 determined by the growth rate of strains in neutralism, cooperation (induced with 25 ng/ ml
747 of nisin) and competition. The ratio of average growth rate of two strains in each consortium
748 is 0.6 (Cooperation): 0.79 (Competition): 1 (Neutralism) in liquid culture. Cooperation with
749 the lowest growth rate formed clear laws on agar after 45 h growth. Then the end point of
750 experiment of the other two ecosystems was calculated based on this time: 35 h (~0.76 of

751 cooperation) for competition and 25 h (~0.6 of cooperation) for neutralism. Acquisition of
752 images was performed with a Zeiss Axio V16 microscope using a HRm camera (Zoom 7×).
753 The colonies grown from the droplets were subsequently picked up with an inoculating loop
754 and dissolved in the PBS buffer. Ratios of strain A and strain B were counted by both plate
755 pouring and flow cytometry. The spatiotemporal patterns of the predation ecosystem were
756 obtained by spotting the well-mixed consortium droplets on the agar and taking images
757 every 12 h with a Zeiss Axio V16 microscope.
758
759 **Spatial patterns of structured consortium droplets.** Overnight cultures were centrifuged
760 and washed once with fresh media. The concentration of cells was diluted to an OD_{600} of
761 0.5 using fresh media. Then 0.5 μl of strain A and strain B in an ecosystem (neutralism,
762 cooperation and competition) was added to a 90-mm agar plate (20 ml of 2% GM17 agar
763 with appropriate antibiotics) with different distances. The plates were incubated at 30°C for
764 different hours (25 h for neutralism, 45 h for cooperation and 35 h for competition).
765 Acquisition of images was performed with a Zeiss Axio V16 microscope using a HRm
766 camera (Zoom 7X).
767
768 **Culture simulations.** A general framework was constructed to describe the population
769 dynamics of any two-strain community where the strains consume a common nutrient and
770 interact through signaling molecules. Well-mixed culture models for six different social
771 interactions (commensalism, amensalism, neutralism, cooperation, competition and
772 predation) were first constructed modularly from the framework. These models were fit to
773 experimental data, then recombined modularly to predict three- and four-strain ecosystems.
774 Whenever possible equations and parameters were reused to reflect the modular
775 construction of the ecosystems. MATLAB was used to produce plots, analyze images and fit

776 data for the models. Data from supplemental control experiments were also used to fit
777 parameters.
778
779 **Spatial simulations.** A general framework was constructed to describe the spatiotemporal
780 dynamics of any two-strain community which involves nutrient co-utilization and active
781 social interactions through diffusible signaling molecules. All three symmetric ecosystems
782 (neutralism, cooperation and competition) were constructed modularly to reflect the modular
783 reconfiguration concept of the ecosystem engineering. Each ecosystem was simulated
784 using C++ and analyzed in MATLAB. The entropy and co-localization of bacterial strains
785 were also measured and plotted.
786
787 **Statistical analysis.** All of the experiments were performed for at least three times.
788 Replicate numbers of the experiments (n) are indicated in the figure legends. Sample sizes
789 were chosen based on standard experimental requirement in molecular biology. Data are
790 presented as mean ± s.d. Fluorescence microscopy images are representatives of the
791 images from multiple experimental replicates.
792
793 **Life Sciences Reporting Summary.** Further information on experimental design is
794 available in the Life Sciences Reporting Summary.
795
796 **Code and Data availability.** Custom C++ and MATLAB codes developed in this study and
797 data supporting the findings of this study are available within the paper and its
798 supplementary information files or from the corresponding author upon reasonable request.
799 Sequences of plasmids are available at GenBank under the following accession numbers:
800 pWK6, MG913135; pWK6-RK^{-}, MG913136; pWK6b-PRK^{-}, MG913137; pWK-lcnA^{wt},

801 MG913138; pWK-lcnA^{5k}, MG913139; pWK-lcnA^{20k}, MG913140; pWK6-IFEG, MG913141;
802 pWK6-IPFEG, MG913142; pWK6-IFEG-lcnA^{wt}, MG913143.
803
804 **References**

805 38. Le Loir, Y., Gruss, A., Ehrlich, S. & Langella, P. A Nine-Residue Synthetic
806 Propeptide Enhances Secretion Efficiency of Heterologous Proteins in *Lactococcus*
807 *lactis*. *J. Bacteriol.* **180**, 1895-1903 (1998).
808 39. Oh, J.-H. & van Pijkeren, J.-P. CRISPR–Cas9-assisted recombineering in
809 *Lactobacillus reuteri*. *Nucleic Acids Res.* **42**, e131 (2014).
810 40. Douglas, G.L. & Klaenhammer, T.R. Directed Chromosomal Integration and
811 Expression of the Reporter Gene *gusA3* in *Lactobacillus Acidophilus* NCFM. *Appl.*
812 *Environ. Micobiol*. **77**, 7365-7371 (2011).
813 41. Fernández, A., Horn, N., Gasson, M.J., Dodd, H.M. & Rodríguez, J.M. High-level
814 coproduction of the bacteriocins nisin A and lactococcin A by *Lactococcus lactis*. *J.*
815 *Dairy Res.* **71**, 216-221 (2004).

816